Proposal and Evaluation of a Parameter free segmented Multistep Algorithm to assess Diffusion Data with a combined IVIM-DKI Model

Moritz C Wurnig[1], David Kenkel[1], Lukas Filli[1], and Andreas Boss[1]
[1]*Institute of Diagnostic and Interventional Radiology, University Hospital Zurich, Zurich, Zurich, Switzerland*

Purpose: Several different models for the signal decay in diffusion weighted imaging (DWI) have been proposed. These include the classical monoexponential model with the apparent diffusion coefficient as free parameter and the quite popular intra-voxel incoherent motion (IVIM) model[1], which includes perfusion effects present at low b-values. Furthermore the diffusion kurtosis (DKI) model was proposed, which takes into account the non-Gaussian diffusion behavior of water molecules at high b-values[2]. As diffusion models are getting more complex fitting of the measured signal decay becomes more unstable with increasing numbers of free parameters, which is especially true for the IVIM model, a fact that greatly hampered the usage of these more complex models. To overcome this issue different approaches have been used and recently a parameter free version of the very commonly used segmented multistep procedure for the IVIM model was proposed[3]. In this study we expanded the proposed parameter free segmented multistep algorithm for a combined IVIM-DKI model of diffusion and evaluated its performance regarding the resulting goodness-of-fit in comparison with the simpler IVIM diffusion model.

Materials and Methods: 6 healthy subjects (4 m/ 2 f; median age 25.5 years; range 23-28 years) underwent MRI examinations of the upper abdomen in a 3 Tesla whole-body MR scanner (Ingenia, Philips, Best, The Netherlands) using the 16-channel flexible anteroposterior phased-array coil. Diffusion data sets were acquired using 16 different b-values (0, 10, 20, 40, 90, 100, 170, 200, 210, 240, 390, 530, 620, 750, 970, 1000 s/mm2) with a spin-echo prepared echo-planar imaging (EPI) sequence in transverse orientation during free breathing. Sequence parameters were: TR 5000 ms, TE 69 ms, slice thickness 5 mm, receiver bandwidth 2321 Hz/px, number of averages 6, matrix size 144 x 144, in-plane resolution 2.8 x 2.8 mm, parallel imaging SENSE factor 2, and SPAIR (spectral selection attenuated inversion recovery) fat suppression. A region-of-interest (RoI) analysis was used to compute signal-intensity curves as a function of the b-value in different abdominal organs including liver, pancreas, spleen and kidneys as well as the erector spinae muscle. The signal decay was fitted using the IVIM diffusion model (S_b/S_0 = Fp×exp(-b×D*)+(1-Fp)×exp(-b×D)) and a combined IVIM-DKI diffusion model (S_b/S_0 = Fp×exp(-b×D*)+(1-Fp)×exp(-b×D+b^2×D^2×K/6)). For fitting we used the recently described parameter free segmented approach[3], which was also extended for usage with the IVIM-DKI-model. Goodness-of-fit for the resulting fitted curves was assessed using Akaike's Information Criterion (AIC). To test for differences between the diffusion models paired Student t tests were used. Furthermore parametrical maps for the different parameters of the assessed diffusion models were computed on a pixel-by-pixel basis.

Results: Mean D values [10^{-3} mm^2/s] significantly increased in all assessed organs when using the IVIM-DKI model (p< 0.02 for all comparisons). This was accompanied by a significant decrease of the AIC in the liver (left and right lobe), the pancreas and the renal medulla indicating a significantly better fitting curve (p<0.02 for all comparisons, cp. Table 1 and Figure 1). Mean D* [10^{-3} mm^2/s], Fp [%] and K values (±standard deviation) were: right liver lobe: 103.2±53.9, 26±5, 1.04±0.25; left liver lobe: 55.8±14.4, 36±6, 1.62±1.06; renal cortex: 19.9±10.3, 36±10, 0.40±0.13; renal medulla: 84.4±51.0, 21±6, 0.50±0.14; pancreas: 65.2±44.0, 27±11, 0.70±0.23; spleen: 75.2±25.1, 14±4, 0.86±0.19; skeletal muscle: 48.4±27.8, 11±5, 0.18±0.18. Parametrical maps for the all free parameters of the evaluated diffusion models could be obtained in appropriate image quality (cp. Figure 2).

	mean D_{ivim} ± SD [10^{-3} mm^2/s]	mean $D_{ivim\text{-}dki}$ ± SD [10^{-3} mm^2/s]	p-value	mean AIC_{ivim} ± SD	mean $AIC_{ivim\text{-}dki}$ ± SD	p-value
Left liver lobe	1.18±0.36	1.54±0.43	<0.001	-107.3±4.8	-109.4±4.9	0.012
Right liver lobe	0.99±0.17	1.21±0.24	0.002	-112.8±6.9	-115.6±8.3	0.006
Pancreas	1.57±0.48	1.87±0.57	0.001	-106.5±4.6	-107.6±4.5	0.003
Renal medulla	1.78±0.12	2.04±0.13	0.001	-115.1±4.6	-116.8±5.2	0.004
Renal cortex	1.69±0.33	1.87±0.32	0.001	-119.2±11.0	-119.0±11.3	0.714
Spleen	0.88±0.09	1.00±0.13	0.002	-114.4±8.0	-114.5±7.7	0.794
Erector spinae muscle	1.45±0.24	1.56±0.26	0.013	-137.3±4.6	-137.2±4.7	0.955

Table 1: Mean D values significantly increased when the combined IVIM-DKI model was used. This was accompanied by a significantly better fitting curve for tissues such as liver and pancreas.

Discussion: Here we present our first results applying an extended version of the recently proposed parameter free segmented multistep algorithm for deriving the free parameters of a combined IVIM-DKI diffusion model. We could show that usage of this model leads to a significantly better fitted signal decay curves in tissues such as liver and pancreas when compared to the simpler IVIM model and therefore conclude that this model more accurately describes the behavior of tissue in diffusion experiments and might be used in the future for more precise tissue characterization without organ specific adaptions.

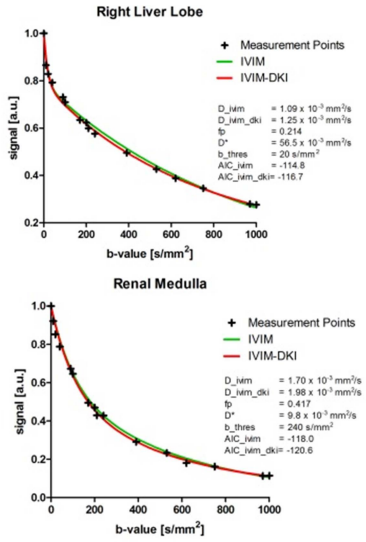

Figure 1: Typical fitted curves for both diffusion models

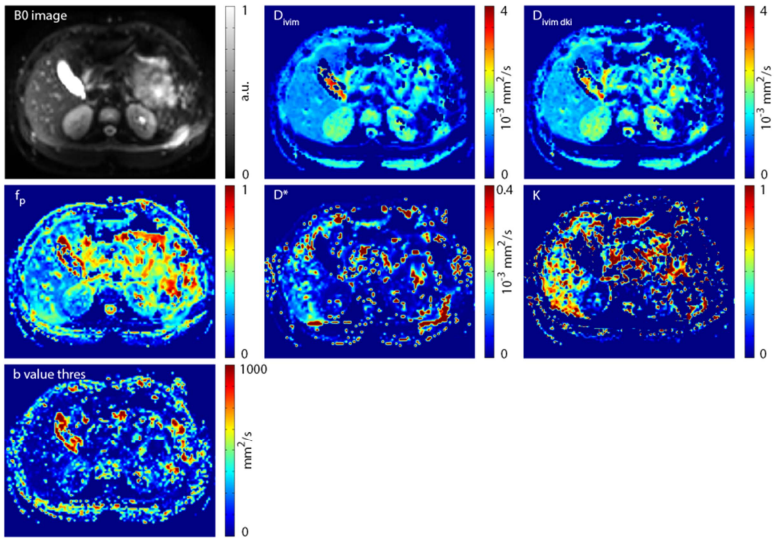

Figure 2: Typical derived parametric maps. Note the increase of D in the liver and the renal medulla when the IVIM-DKI model is used

References:
[1] Le Bihan D, Breton E, Lallemand D, Grenier P, Cabanis E, Laval-Jeantet M. MR imaging of intravoxel incoherent motions: application to diffusion and perfusion in neurologic disorders. Radiology 1986;161(2):401-407.
[2] Jensen JH, Helpern JA, Ramani A, Lu H, Kaczynski K. Diffusional kurtosis imaging: the quantification of non-Gaussian water diffusion by means of MRI. Magn. Reson. Med. 2005; 53: 1432–1440.
[3] Wurnig MC, Donati OF, Ulbrich E, Filli L, Kenkel D, Thoeny HC, Boss A. Systematic analysis of the intravoxel incoherent motion threshold separating perfusion and diffusion effects: Proposal of a standardized algorithm. Magn Reson Med. 2014 Oct 31. doi: 10.1002/mrm.25506. [Epub ahead of print].